A NUMERICAL APPROACH FOR ANALYZING POST-IMPACT BEHAVIOUR OF COMPOSITE LAMINATE PLATE UNDER IN-PLANE COMPRESSION

C. CHEN[1*], C. ESPINOSA[1], L. MICHEL[1], F.LACHAUD[1]

[1]*Université de Toulouse, ISAE, ICA (Institut Clément Ader), 10 av. E. Belin, 31055 Toulouse, France*
** cheng.chen@isae.fr*

Keywords: Compression after impact, Composite laminate, Finite element analysis, Continuum damage mechanics model.

Abstract
This article introduces a numerical method for compression after impact simulation for 150x100mm² composite laminate specimen made from T800S/M21 with impact damage. A continuum damage model has been developed at ICA-ISAE which describes impact damage by material module reduction through six damage variables, and the contribution of different ruin modes on each one. Each damage variable is obtained by summing the contribution of 5 different ruin modes (fiber breakage in tension or compression, spherical crush, perpendicular and parallel matrix cracking). This model was used to predict impact damage. The numerical computation of CAI is performed with this damage model based on the computed realistic impact damage. The evolution and competition of different impact damage and ruin modes during CAI can be monitored and analyzed to determine which is predominant in the final rupture of the sample. At the same time, CAI tests are conducted on specimens impacted at 15J 20J and 30J with the purpose of validation. Some specimens were unloaded just before the final rupture to preserve of first initiated damage which could be identified by X-ray and C-scan examination.

1 Introduction

Composite materials are used increasingly in aeronautical and aerospace applications due to its high strength and stiffness characteristics combined with low density. However, the weak point of laminated composite structures are particularly the out-of-plane strength and the susceptibility to damage induced by low energy impact in BVID (Barely Visible Impact Damage) level which might be overlooked by a regular inspection. This impact induced damage which typically takes the form of fiber breakage, matrix cracks and delamination could dramatically degrade structural strength (60% reduction or more in compression) and structural stiffness as well [1,5]. Thus accurate and efficient methods to predict the residual mechanical properties of laminated composite structure are important and necessary for the design of structure with consideration of damage tolerance.

Numerous articles were dedicated to the study of impact and CAI behaviors of laminated composite panel in the research community. The creation of impact damage in the numerical model plays a critical role in CAI calculation. Various methods have been proposed with the consideration of impact damage as equivalent hole, soften region, delamination opening which are idealized and simplified compared to the real case. Thus, due to this damage

assumption, the structural response and damage evolution might not be accurately reproduced in CAI.
This article describes first a Continuum Damage Model which is developed in DMSM-ISAE ICA. This material model is implemented in LS-Dyna, and good results are achieved for impact damage prediction [2]. The numerically predicted realistic 3D impact damage is preserved and then used directly as an initial damage for the CAI computation. By analyzing and comparing the evolution of different damage variables and damage modes, it's possible to determine the first propagated damage and distinguish the competition of different damage modes when the material degrades.
Seven specimens impacted by different energy levels (10J, 20J, 25J, 30J) are available for CAI test. An innovative unloading technique is employed which helps preserve first initiated damages before final rupture so that it could be possible to identify which damage pattern initiates first.

2 Material damage model

Based on a thermodynamics material model presented in [3], Dr.ILYAS derived specific failure criteria for T800S/M21 aeronautical laminates subjected to impacts [2]. It takes into account the degradation of material by manipulating 6 damage variables $\{d_i\}$ i=1,6 which bring a progressive loss to material elastic rigidity (eq-1).

$$E_i = E_i^0 \cdot (1 - d_i) \qquad \text{(eq-1)}$$

where E_i is damaged elastic module, and E_i^0 is its initia value
Damage variables are computed as the sum of damage contribution $\{\phi_j\}$j=1,5 from 5 ruin modes through a coupling matrix $\{q_{ij}\}$ i=1,6 j=1,5 (eq-2). $\{\phi_j\}$ is a function of ruin mode $\{r_j\}$ j=1,5 defined by the failure criteria $\{f_j\}$ and m_i which is a material parameter affecting damage evolution in each damage mode (eq-3).

$$\begin{Bmatrix} d_1 \\ d_2 \\ d_3 \\ d_4 \\ d_5 \\ d_6 \end{Bmatrix} = \begin{bmatrix} 1 & 1 & 1 & 0 & 0 \\ 0 & 0 & 1 & 1 & 0 \\ 0 & 0 & 1 & 0 & 1 \\ 1 & 1 & 1 & 1 & 1 \\ 0 & 0 & 1 & 1 & 1 \\ 1 & 1 & 1 & 0 & 1 \end{bmatrix} \times \begin{Bmatrix} \phi_1 \\ \phi_2 \\ \phi_3 \\ \phi_4 \\ \phi_5 \end{Bmatrix} \qquad \text{(eq-2)} \qquad \phi_j = 1 - e^{\frac{1}{m_j}\left(1 - r_j^{m_j}\right)} \qquad \text{(eq-3)}$$

The five damage criteria are described in following eq (4-8). They have been derived through an experimental classical quasi-static characterization of the T800S/M21 and T700S/M21, and dynamic testing [2]. Strain rate effects were identified as well and are represented by the regression function of (eq-9).

Tension/shear failure criterion

$$f_1(\sigma, \omega, r) = \left(\frac{\langle \sigma_{11} \rangle}{X_T}\right)^2 + \left(\frac{\sigma_{12}^2 + \sigma_{13}^2}{S_{fs}^2}\right) - r_1^2 = 0 \qquad \text{(eq-4)}$$

Compression failure criterion

$$f_2(\sigma,\omega,r)=\left(\frac{\left\langle -2\sigma_{11}+\left\langle -\sigma_{22}-\sigma_{33}\right\rangle\right\rangle}{2X_c}\right)^2-r_2^2=0 \qquad \text{(eq-5)}$$

Matrix crushing criterion

$$f_3(\sigma,\omega,r)=\left(\frac{\left\langle -\sigma_{11}-\sigma_{22}-\sigma_{33}\right\rangle}{3Z_C}\right)^2-r_3^2=0 \qquad \text{(eq-6)}$$

Matrix transverse failure criterion

$$f_4(\sigma,\omega,r)=\left(\frac{\langle\sigma_{22}\rangle}{X_C}\right)^2+\left(\frac{\langle\sigma_{22}\rangle}{Y_C}\right)^2+\left(\frac{\sigma_{12}}{S_{12}+\langle-\sigma_{22}\rangle\tan\varphi}\right)^2+\left(\frac{\sigma_{23}}{S_{23}+\langle-\sigma_{22}\rangle\tan\varphi}\right)^2-r_4^2=0 \qquad \text{(eq-7)}$$

Matrix parallel failure criterion (Delamination)

$$f_5(\sigma,\omega,r)=\left(\frac{\langle\sigma_{33}\rangle}{Z_T}\right)^2+\left(\frac{\sigma_{13}}{S_{13}+\langle-\sigma_{33}\rangle\tan\varphi}\right)^2+\left(\frac{\sigma_{23}}{S_{23}+\langle-\sigma_{33}\rangle\tan\varphi}\right)^2-r_5^2=0 \qquad \text{(eq-8)}$$

where $\tan\varphi$ takes into account the effect of friction on shear when the ply is under transverse compression.

$$\sigma_{ij}=\sigma_{ij}^{Sta}\left(1-C_i\ln\frac{\dot{\varepsilon}}{\dot{\varepsilon}_{ref}}\right) \qquad \text{(eq-9)}$$

The six stress components determine the evolution of damage mode value r_i . Once r_i becomes greater than its initial value of 1, its corresponding damage mode initiates, and contributes to the accumulation of its coupled damage variables.

3 Experiments

3.1 Specimen preparation

All laminates were manufactured from T800S/M21 carbon/epoxy prepreg(UD/M21/35%/268/ T800S/300) and auto-clave-cured according to the supplier's recommendations (Hexcel). Prior to machining, the laminates were examined for internal defects using ultrasonic C-Scan technique. The results indicate that the specimens are of good qualities. Test specimens measuring 150mm by 100mm were cut out from panels.

The stacking sequence tested is [-45/+45/0/90/0_2/-45/+45/0]s, which is a strongly oriented, middle plane symmetric ,18-ply layup.

$E_l=165Gpa \quad E_l=E_t=7.69Gpa \quad E_z=7.69Gpa \quad G_{lz}=G_{lt}=4.75Gpa \quad G_{tz}=2.75Gpa$

$\upsilon_{lz}=\upsilon_{tz}=0.33 \quad \upsilon_{tz}=0.4$

Table 1. Material properties of T800S/M21 for one ply

3.2 Impact test

The drop tower setup is used for impact tests. The impactor equipped with a load cell is dropped from a distance above the specimen calculated from predefined impact energy. A 16mm diameter hemispherical head made of harden steel which weighs 2.369kg is installed

on the impactor. Impact tests are performed with 4 energy levels: 10J, 20J, 25J, 32J. More energy levels in [2].
The specimens are placed on a 300mmx200mm steel support which is fixed to a rigid frame. This support contains a 125mmx75mm rectangular cut-out allowing a free deformation when specimen responses to impact load.
After impact tests, all specimens passed through ultrasonic "time-of-flight" C-Scan, X-ray and visual examination for non-destructive characterization of internal damage. Besides, permanent indentation was also measured just after impact and 48h later.

3.3 Compression after impact
Subsequent to non-destructive characterization of impact damage, compression after impact test is performed with an Instron® hydraulic universal test system with a capacity of $\pm 25KN$,Figure-1(left). A CAI fixture, shown in Figure-1(right), which conforms ASTM D7137/D7137M standard is used. This fixture provides simple supports on two vertical edges so that global buckling could be avoided. Tests were achieved at a constant load rate of 5KN/min. The loading and support edges are clamped to avoid end "brooming".

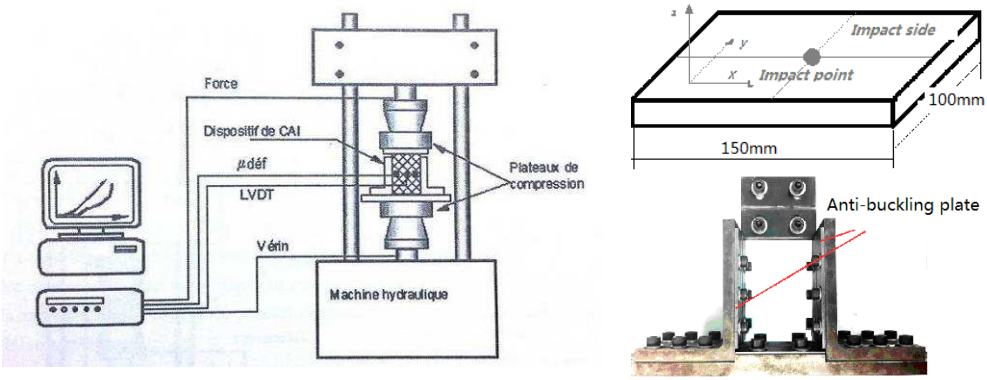

Figure.1 Compression test system (left) compression fixture (right)

One LVDT (Linear Variable Differential Transformer) and a Stereo Image Correlation device (with two cameras) are installed at the impact and non-impact side respectively for out-of-plane displacement measurement. Two acoustic sensors are installed on impact side of the specimen to monitor damage initiation and evolution by collecting acoustic signals due to material degradation.
Besides, in order to capture the damage initiation before the final failure, an unloading technique is attempted here. This method is based on the real-time acoustic monitoring. Several specimens are loaded to final failure on purpose to get a reference of acoustical signal number before final failure. With the reference, several specimens are unloaded when the occurrence of the first initiated damage when a certain number of acoustic signals are detected. As shown in Figure-2 (left), acoustic signals are detected and monitored for a 20J impacted CAI test. Four positions A, B, C and D are marked. Internal damage translated as acoustic signals started developing from position B. After a slow evolution, from position C acoustic signals increase more rapidly until about 150 hits at position D. This implies internal damage has evolved dramatically before final CAI failure. The critical hit number -150 refers to acoustic hit number for ruptured specimens. On the non-impact surface, a local buckling of detached last ply with double coconut shape is first observed from position B to C, Figure-2(right). Then from position C to D, a consequent local plate buckling form reveals. These deformations are accompanied by irreversible internal damage implied by acoustic detection.

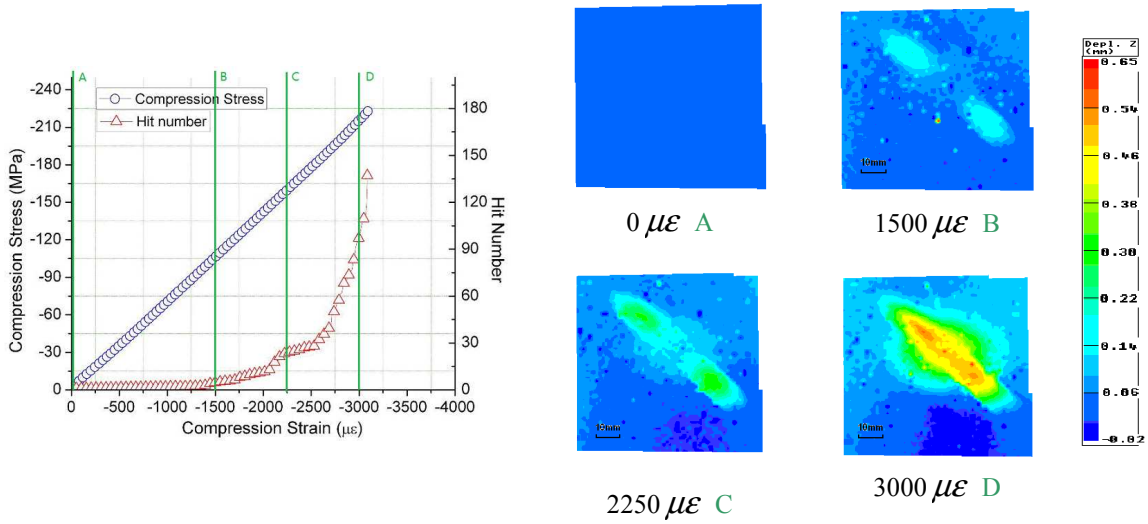

Figure 2 Acoustic number detected (left) non-impact side out-of-plane deformation (right) (20J)

4 Simulation

The Continuum Damage Model (CDM) implemented as a user-defined subroutine in LS-Dyna® is used to obtain 3D impact induced damage configuration using explicit simulations. A restart technique of LS-Dyna is used to use the final state of this run as the initial state of the compression simulation Compression calculation are then performed by preserving calculated realistic 3D impact damage. This method allows exploring CAI behaviors with realistic damage configuration instead of a presumed simple one. A much more precise consideration of impact damage should lead to a better CAI behavior prediction.

Besides, the specimen gained kinetic energy from impact which takes the form of strong vibration. This vibration was eliminated so that it wouldn't affect specimen response to post-impact compression.

To compromise between dynamic loading effect and calculating time, a compression loading rate of 0.2mm/ms is prescribed on loading edge.

5 Comparison between CAI test and Numerical calculation

Figure-3(left) shows a comparison of strain-stress curve of theoretical calculation, experiment and simulation for the case of 20J impact. The four experimental curves show that specimens fail in a brutal way, while simulation computed CAI stress vs. strain curve consists of three stages: linear, non-linear and after failure. Failure takes place in a progressive softened way.

5.1 Residual rigidity

The theoretical value of equivalent modulus in loading direction for a ''healthy'' specimen is calculated as a reference based on classical laminate theory, [4]. The simulation equivalent modulus is calculated based on the linear part of stress vs. strain curve. The experimental and simulation values fell below the theoretical one as a result of impact damage induced rigidity loss. However experimental values are more dispersed than simulation values, Figure-3(right). Compared to experimental values, the equivalent modulus seems underestimated in the simulation. This might be due to the fact that delamination which doesn't reduce rigidity before buckling is represented by rigidity loss in this damage model.

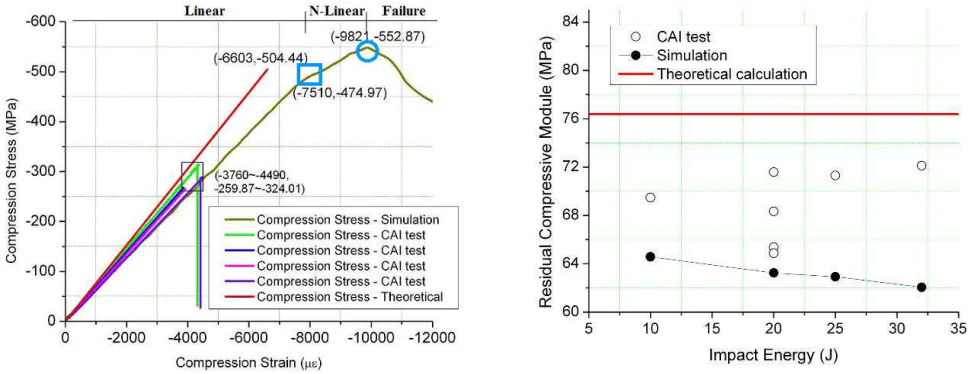

Figure.3 Comparison of CAI test, simulation, theoretical (20J) (left) Comparison of equivalent modulus (right)

5.2 First damage initiation

The damage variable d_4 comprises the contribution of all 5 damage modes so that it could be seen as a representation of internal damage.

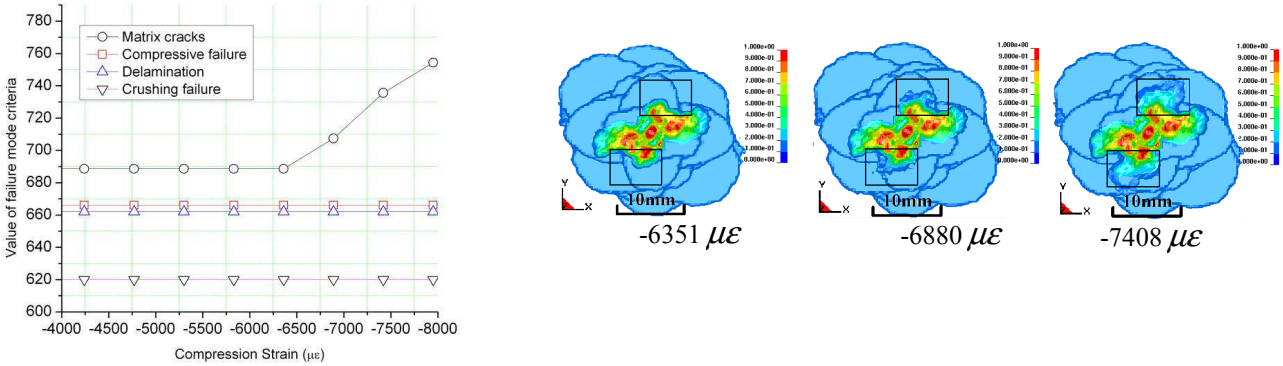

Figure.4 Contribution of failure criteria (left) damage variable d_4 (right) (20J)

In order to identify the first propagation of internal damage in CAI simulation, the plotting of d_4 is monitored at each time step. It turns out that a first propagation of internal damage is observed at the first ply near to impact side when the compression strain reaches -6351 $\mu\varepsilon$. The propagation zone is located within black rectangles marked in Figure-4 (right). It's worth noting that the propagation direction is perpendicular to the loading direction but a little bit diverted to 45 degree direction.

The values of failure mode criteria for each element in the first ply included in the captured area are summed and plotted in Figure-4(left). It clearly shows the first initiated damage is matrix cracks from -6351 $\mu\varepsilon$, while other failure criteria don't change a bit.

To verify experimentally the first initiated damage, ultrasonic C-Scan examination is done for specimens which were successfully unloaded. Comparing the C-Scan examining result between before and after compression, no measurable damage propagation is observed. But the more interesting fact is the appearance of some white zones, Figure-5(left and middle)

On the non-impact side, the white zone shape conforms well the last ply local buckling shape Figure-5(middle). This implies the out-of-plane deformation due to local buckling causes a dispersion of signal reflection which couldn't be received anymore, Figure-5(right). On the impact side, the white zone appears in a thickness range between 0mm to 1mm. However, it's difficult to tell the cause of white zone. It could be due to the formation of massive 45 degrees matrix cracks which diverse ultrasonic signals or considerable opening of inner delaminations which attenuates and diverse ultrasonic signal. A micro-observation on several cutting sections is studied with purpose of validating these assumptions. However, due to limited

specimen number, it's difficult to confirm such conclusions for this moment. A series of CAI tests is in progress for investigation of this phenomenon.

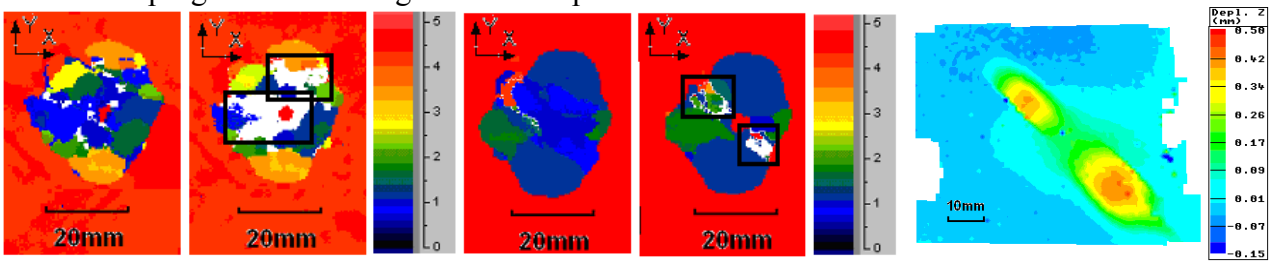

Figure. 5 C-Scan comparison impact side (left), non impact side (middle) C-Scan non impact side (right) (20J)

5.3 Damage Evolution

CAI Stress vs. strain curve of 20J impacted specimen is marked with different letters representing different stages, Figure-6(left). From state C, damage starts diffusing in all plies in a much more rigorous way than the initiation stage. After peak value (state H) in the stress vs. strain curve is reached, specimen enters the rupture phase. Damage develops even faster until it reaches saturation at state L, Figure-6(right). Compared with C-Scan result, internal damage d4 plotting corresponds well the real damage band shape. The calculated damage band width 36.07mm is very close to the CAI test one which measures 35.01mm.

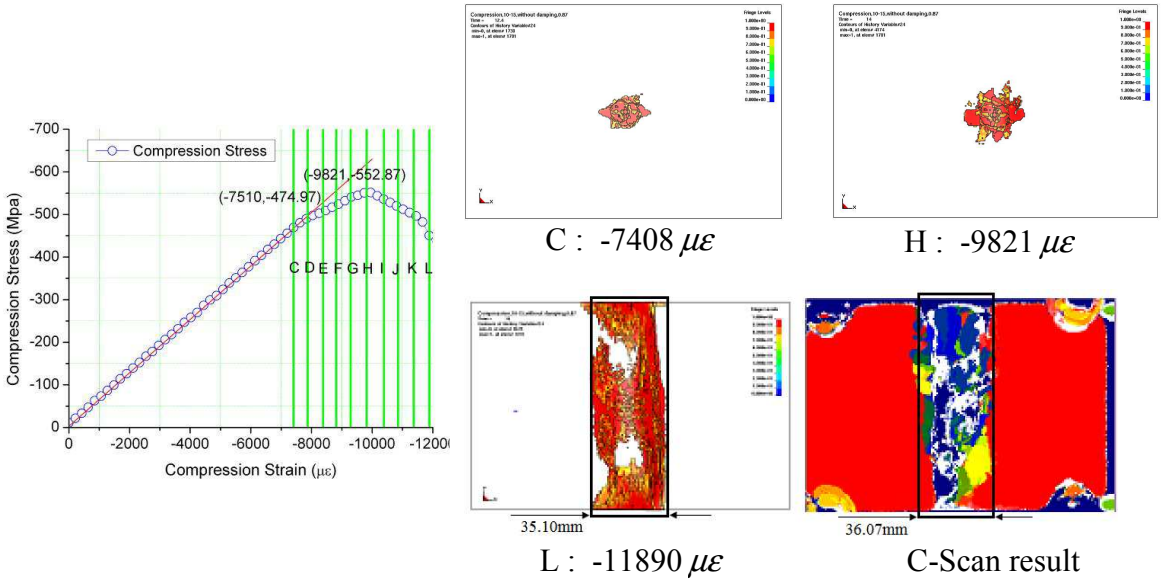

Figure.6 Stress vs. strain (left) Damage plotting of d4 (right) – 20J

In Figure-7, maximum damage values in each ply for fiber compressive failure (r2), matrix failure (r4) and delamination failure (r5) are plotted (fiber traction failure r1 and crush failure r3 don't evolve) to capture the damage mode evolution. From -7510 $\mu\varepsilon$ to -9821 $\mu\varepsilon$, it is fiber compressive failure mode which gives the greatest contribution to the internal damage d4. In other 4 failure modes, their maximum failure mode value in each ply isn't exceeded.

After the maximum failure compression stress is reached, internal damage propagates with contributions mainly from fiber compression failure, matrix failure and delamination failure. However, compared to matrix failure, delamination and fiber compression failure play a much more important role in advancing the internal damage.

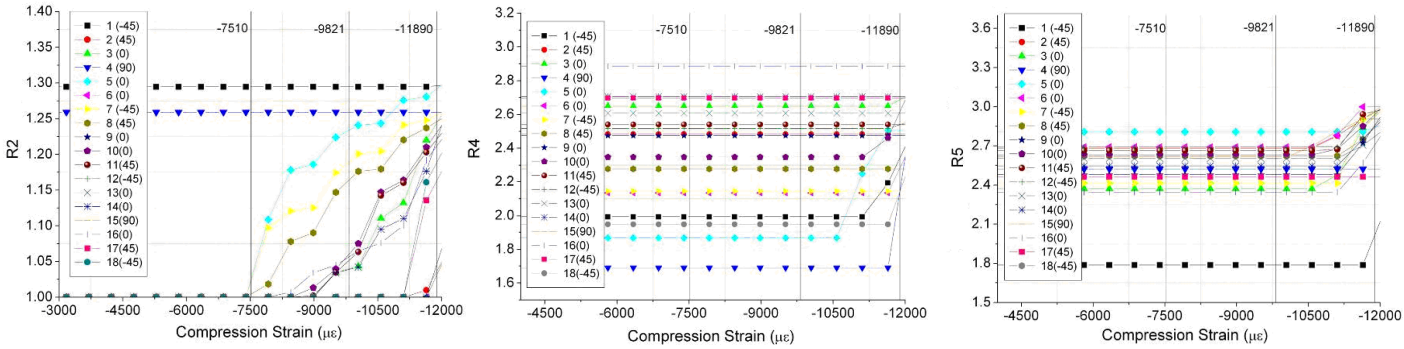

Figure.7 Evolution of damage modes r2, r4, r5

6 Conclusions

This article realizes a numerical strategy with which CAI simulation could be performed with a realistic 3D damage configuration obtained from last state of impact simulation. The estimation of residual compressive equivalent modulus is slightly underestimated. Numerical result implies that first initiated damage is due to matrix cracks in the first ply impact side and it propagates in the ply direction. Limited specimen number couldn't lead to a convinced conclusion on this observation in calculation. A series of CAI tests is in progress for further confirmation. The propagation of impact damage is contributed by matrix cracks, delamination and compressive failure, and the latter two seem to be more important in advancing impact damage. Damage zone at rupture failure is well predicted in terms of shape and dimension. With the help of acoustic detection, an innovative unloading technique developed in this article works well in preserving a first propagated impact damage during CAI.

References

[1] Abrate, S. (1991). Impact on laminated composite materials. Applied Mechanics Reviews, 44: 155-190.

[2] Ilyas.[2010] Damage modeling of carbon epoxy laminated composites submitted to impact loading, PhD thesis, ISAE

[3] Matzenmiller, A., Lubliner, J., and Taylor, T.L. (1995). A constitutive model for anisotropic damage in fber-composites. Mechanics of Materials, 20(2):125-152

[4] Gay, D. (1997). Matériaux composites. Hermès, 4ème edition

[5] Aboissiere, J. (2003). Propagation de dommages d'impact dans un materiau composite stratifié a fibres de carbonne et résine époxyde. PhD thesis, ISAE